DOE Final Technical Report
DE-FG02-03ER6362

Summary

Although radiation-induced heritable damage in mammalian cells was thought to result from the direct interaction of radiation with DNA, it is now accepted that biological effects may occur in cells that were not themselves traversed by ionizing radiation but are close to those that were. However, little is known about the mechanism underlying such a bystander effect, although cell-to-cell communication is thought to be of importance. Previous work using the Columbia microbeam demonstrated a significant bystander effect for clonogenic survival and oncogenic transformation in C3H 10T(1/2) cells. Additional studies were undertaken to assess the importance of the degree of cell-to-cell contact at the time of irradiation on the magnitude of this bystander effect by varying the cell density. When 10% of cells were exposed to a range of 2-12 alpha particles, a significantly greater number of cells ($P < 0.0001$) were inactivated when cells were irradiated at high density (>90% in contact with neighbors) than at low density (<10% in contact). In addition, the oncogenic transformation frequency was significantly higher in high-density cultures ($P < 0.0004$). These results suggest that when a cell is hit by radiation, the transmission of the bystander signal through cell-to-cell contact is an important mediator of the effect, implicating the involvement of intracellular communication through gap junctions.

Additional studies to address the relationship between the bystander effect and the adaptive response were undertaken in order to ascertain the competitive impact of the two effects on the dose-response curve at low doses. A novel radiation apparatus, where targeted and non-targeted cells were grown in close proximity, was used to investigate these phenomena in C3H 10T(1/2) cells. It was further examined whether a bystander effect or an adaptive response could be induced by a factor(s) present in the supernatants of cells exposed to a high or low dose of X-rays, respectively. When non-hit cells were co-cultured for 24 h with cells irradiated with 5 Gy alpha-particles, a significant increase in both cell killing and oncogenic transformation frequency was observed. If these cells were treated with 2 cGy X-rays 5 h before co-culture with irradiated cells, approximately 95% of the bystander effect was cancelled out. A 2.5-fold decrease in the oncogenic transformation frequency was also observed. When cells were cultured in medium donated from cells exposed to 5 Gy X-rays, a significant bystander effect was observed for clonogenic survival. When cells were cultured for 5 h with supernatant from donor cells exposed to 2 cGy and were then irradiated with 4 Gy X-rays, they failed to show an increase in survival compared with cells directly irradiated with 4 Gy. However, a twofold reduction in the oncogenic transformation frequency was seen. An adaptive dose of X-rays cancelled out the majority of the bystander effect produced by alpha-particles. For oncogenic transformation, but not cell survival, radioadaption can occur in unirradiated cells via a transmissible factor(s).

A pilot study was undertaken to observe the bystander effect in a realistic multicellular three-dimensional morphology. Given that the bystander phenomenon must involve cell-to-cell interactions, these studies are of great interest. We found bystander responses in a three-dimensional, normal human-tissue system. Endpoints were induction of micronucleated and apoptotic cells. A charged-particle microbeam was used, allowing irradiation of cells in defined locations in the tissue yet guaranteeing that no cells located more than a few micrometers away

receive any radiation exposure. Unirradiated cells up to 1 mm distant from irradiated cells showed a significant enhancement in effect over background, with an average increase in effect of 1.7-fold for micronuclei and 2.8-fold for apoptosis. The surprisingly long range of bystander signals in human tissue suggests that bystander responses may be important in extrapolating radiation risk estimates from epidemiologically accessible doses down to very low doses where nonhit bystander cells will predominate.

Finally, in order to be able to extrapolate the in vitro results to in vivo models with confidence, it would be of great benefit to develop a reproducible tissue system suitable for critical radiobiological assays. We have developed a reliable protocol to harvest cells from tissue samples and to investigate the damage induced on a single cell basis. In order to result in a valid tool for bystander experiments, the method focuses on processing and analyzing radiation damage in individual cells as a function of their relative position in the tissue. We have investigated the micronucleus formation following partial irradiation with 3.5 MeV protons (<10 keV/μm) in an artificial human skin construct (EpiDermTM) engineered by MatTek Corp. (Ashland, MA, USA). Following the optimization of the Cytochalasin-B concentration and incubation time necessary to obtain a reproducible and suitable number of binucleated cells (>60% for 3 μg/μl after 48h), the induction of micronuclei across the samples is assessed for 3 dose points (0.1, 0.5 and 1 Gy). The reproducible and low background frequency of micronuclei measured in this system allowed us to detect small increases following the irradiation exposure. The effect is statistically significant at doses as low as 0.1 Gy and it shows evidence of a spatial dependency as it decreases in the cells further away from the directly exposed area. This experimental protocol represents the initial steps in the development of an in vivo-like assay for complex radiation damage, such as chromosomal aberrations, in human tissues.

I. The bystander response: The influence of cell-to-cell contact

INTRODUCTION

It has been a long-held tenet of radiation biology that cellular DNA damage required direct interaction of radiation with DNA. This "targeted" DNA damage occurred either by direct ionization or by production of hydroxyl radicals in water molecules adjacent to DNA. However, over the past decade, considerable evidence has emerged for the existence of a "non-targeted" phenomenon that has been termed the bystander effect. The bystander effect is defined as the observation of a biological response in cells which have not been directly traversed by ionizing radiation but which results from signals initiating in cells in which energy has been deposited. This may be an important phenomenon influencing the shape of the dose–response curve, particularly at low doses, where there are many nontraversed cells, and several models are available which assess the significance of such effects at low doses. Although the effect of such bystander responses on the low-dose cancer risk is not fully understood, they are thought to represent a balance between protective mechanisms such as apoptosis and differentiation and potentially harmful mechanisms, in which DNA damage and potential genomic instability are mediated through bystander signals.

To date, many studies, primarily using single cell *in vitro* systems but also *in vivo,* have confirmed a bystander response for several end points including clonogenic survival, oncogenic transformation, micronucleus induction and gene expression. These studies have employed three distinct protocols: the conventional irradiation of cells with low fluences of α particles, the transfer of medium from irradiated onto unirradiated cells, and the use of charged-particle microbeams, which have made it possible to define precisely which cells are traversed by an exact number of α particles. However, the specific factor(s) produced by irradiated cells responsible for the bystander response remains unknown, although several candidate molecules have been suggested

It seems likely that the bystander effect is mediated by two distinct mechanisms that depend on the experimental protocol employed and that both may contribute to the final response. The first involves the transmission of a secreted, soluble extracellular factor from irradiated to unirradiated cells, often over some considerable distance. The second is direct communications between adjacent cells through gap junctions.

Previous studies using the Columbia microbeam have shown a significant bystander effect for the end points of clonogenic survival and oncogenic transformation in C3H 10T½ cells. The aim of the present study was to assess whether the magnitude of this effect was dependent upon cell-to-cell proximity at the time of irradiation. To achieve this, cells were plated at both high and low density, targeted with a range of α particles aimed at the centroid of the nucleus, and assessed for clonogenic survival and oncogenic transformation.

MATERIALS AND METHODS

Microbeam Irradiation

The Columbia microbeam system and the irradiation procedures have been described in detail previously. Briefly, cells were attached to the thin bases (3.8 μm polypropylene) of 6.3-mm-diameter miniwells to give a final cell density of either 200 or 2000 cells per well. Individual nuclei were then identified and located with a computer-controlled optical image analysis system. For each dish, a computer/microscope-based analysis system first automatically locates and records the *x*,*y* coordinates of the nuclei of cells on the dish. Next the dish is moved sequentially under computer control such that the first cell nucleus is positioned over a highly collimated α-particle beam. The beam shutter is opened until the required numbers of α particles are detected (with a gas-filled ion counter mounted on the microscope lens) to have passed through the nucleus. The shutter is then closed and the next cell is moved over the beam. The overall spatial precision of the beam, including positioning and beam spread, is about ±3.5 μm, compared with an average nuclear cross-sectional area of the cells of approximately 200 μm^2 and a cellular cross- sectional area of >500 μm^2. In the present study, 5.3 MeV α particles accelerated by a Van de Graaff accelerator were used for the irradiations. The average stopping power of the α particles traversing the cells was 90 keV/μm. The search and irradiate software can be instructed to expose any given proportion of the cells, selected at random, to any desired number of α particles. To assess clonogenic survival, either 10% or 100% of the cells were exposed to a range of α particles from 2–12 through the nucleus and for oncogenic transformation 10% of the cells were exposed to 8 α particles. Dishes used to assess plating efficiency were sham-irradiated, i.e. handled in an identical fashion except that the beam shutter was not opened. Irradiation times for each dish were approximately 6–10 min.

Cell Culture

Prior to irradiation, C3H 10T½ mouse fibroblast cells between passages 9 and 11 were grown in Eagle's basal medium supplemented with 10% FBS and penicillin/streptomycin. Eighteen hours before exposure, 200 or 2000 exponentially growing cells were plated into miniwells as described above. Prior to irradiation, cells plated at the high density formed a confluent culture with a high degree of cell-to-cell contact, in contrast to the low-density cultures in which the cells were individuals, separated from their neighbors. The attached cells were stained for 0.5 h with 50 n*M* of the vital nuclear dye Hoechst 33342, enabling individual nuclei to be identified and located using the optical image analysis system. Immediately prior to irradiation, cells were washed with serum-free medium to avoid fluorescence from serum components and irradiations were carried out in the presence of a thin film of serum-free medium. After irradiation, cells were washed twice with PBS and trypsinized from the irradiation container. For assessment of clonogenic survival, approximately 100 viable cells were plated into 100-mm culture dishes and incubated for 2 weeks, and the resulting colonies were stained with 2% crystal violet to determine both the plating efficiencies and surviving fractions of the control and irradiated cells. To assess oncogenic transformation, cells were replated at a low density of about 300 viable cells per dish. The cells were incubated for 7 weeks with culture medium changed every 12 days before they were fixed and stained with Giemsa to identify morphologically transformed type II and III foci, as described elsewhere.

Data from a minimum of three independent experiments were pooled. All data for clonogenic survival were presented as means with standard errors. Surviving fractions measured at the doses tested were fitted with the linear-quadratic equation. The statistical significance of differences between groups was tested by Student's *t* test and between survival curves using multiple regression analysis.

RESULTS

The results of the experiments to compare clonogenic survival for cells exposed at high and low density are shown in Fig. 1. The clonogenic survival obtained when 100% of cells are hit by various numbers of α particles is indicated by the solid triangles and is in agreement with that seen previously in C3H 10T½ cells.

The dotted line shows the percentage of the cells that would be expected to survive when 10% of the cells are irradiated in the absence of any bystander effect. It is calculated by applying the 100% survival curve to the 10% of cells that were actually irradiated. The results are compared with those obtained from the irradiation of 10% of the cells at either high or low density, which are shown by the solid circles and squares, respectively. The extent to which these lines fall below the dotted line indicates the magnitude of the bystander effect, although only the cell survival observed in high-density cultures is significantly lower ($P < 0.0001$ compared to $P = 0.11$ at low density). At both cell densities, the surviving fractions fall progressively as more α particles traverse the nucleus, but the amount of cell killing is significantly greater at the high cell density compared with low- density cultures ($P < 0.0001$).

Results from experiments conducted to evaluate the effect of cell density at the time of irradiation on oncogenic transformation are shown in Table 1. In these studies, a total of approximately 3.1×10^5 cells were individually imaged, positioned and irradiated. At high density, a transformation frequency of $9.6/10^4$ viable cells was seen, which is similar to that found previously in high-density cultures. Using previously published data, it is possible to calculate that when 10% of the cells in a population are irradiated with 8 α particles, the expected transformation frequency in the absence of a bystander effect would be $2.1/10^4$ viable cells. This is lower than that seen in the present study at both cell densities, although again the difference is only significant in the case of the high-density cultures ($P < 0.0001$ compared to $P = 0.28$ at low density). A statistically significant threefold decrease in the transformation frequency was observed in the low-density cultures relative to high-density cultures ($P < 0.0004$).

DISCUSSION

It is now widely accepted that radiation-induced heritable effects in mammalian cells are not solely the result of direct damage to DNA, and there is now evidence for a number of non-

targeted effects, including the bystander response, which do not require a direct nuclear exposure.

Although reproducible bystander effects have now been demonstrated for a range of biological end points, the mechanisms by which the biological insult is transmitted from targeted to non-targeted cells have not been fully elucidated).

One causative agent may be the secretion from irradiated cells of a soluble factor(s) into the medium that then elicits a biological response in adjacent, unirradiated cells. Alternatively, when densely cultures are irradiated, the signal may be transmitted through cell-to-cell communication between adjacent cells. When cells are in close contact, they can communicate through gap junctions which are intercellular membrane channels that permit the direct exchange of small molecules (<1.2 kDa) between adjacent cells.

It now seems apparent that for a given cell line, transmission of the bystander signal by cell-to-cell contact elicits a more pronounced bystander effect compared with the transfer of an extracellular factor through the medium, suggesting that these are two separate phenomena. Evidence for this comes from mutation studies in A_L cells using two different protocols. Either 20% of densely cultured cells (≈70% of cells in contact) were irradiated with the Columbia microbeam, or cells on one surface of a double Mylar dish were irradiated while cells on the other side of the dish acted as bystanders. The results suggest that the cytotoxic factor(s) released from the cells into the culture medium using the latter protocol had a small, barely significant effect on the mutagenic response of the bystander cells, whereas the microbeam-based studies showed a threefold elevation of mutation incidence in bystander cells, which was significantly reduced in the presence of the gap junction inhibitor lindane.

A similar conclusion has been implied from experiments performed with V79 cells in two different laboratories. In one study carried out at Columbia University, cells were irradiated with various numbers of α particles and a considerable degree of cell killing was seen in non-hit cells, with survival reduced to 60% at the highest dose of 16 α particles per nucleus. This was in contrast to data from the Gray Cancer Institute, UK, where only 5 to 10% lethality was seen (B. Michael, personal communication, 2001), and it was concluded that this discrepancy was a result of the cells being plated at a lower density in the latter study. Here there was little contact between cells, and therefore the bystander effect observed was assumed to be due to the release of a soluble factor into the medium affecting nonirradiated cells.

However, there are several differences between the protocols used at Columbia and the Gray Cancer Institute for microbeam experiments that, in addition to the cell density at the time of irradiation, may have contributed to the observed discrepancy in survival.

The present study is the first to examine the effect of cell density under the same experimental conditions, allowing us to conclude that any observed differences are solely a result of cell density at the time of irradiation. When approximately 2000 cells were plated on a microbeam dish, the vast majority (>90%) of the cells were in direct contact with neighbors through membranes and intercellular gap junctions when they were irradiated 18 h later. In contrast, when 200 cells were plated using the same protocol, very little contact between cells (<10%) was

seen, with the majority of cells appearing as isolated entities, separated by many tens of micrometers from their neighbors.

The results of the present study confirm those seen previously in C3H 10T½ cells when irradiation of 10% of the cells (≈80% confluent at time of irradiation) on a dish with an exact number of α particles (>4 α particles/nucleus) resulted in a surviving fraction of less than 90%, indicative of a substantial bystander effect.

In the present study, at both high and low cell density, the surviving fraction fell progressively as the number of α particles traversing 10% of the cells increased. This suggests that as more damage is inflicted on the cells, there is an increase in transmission of the bystander signal either through increased gap junction communication (high density only) or increased secretion of a cytotoxic factor(s) into the culture medium. However, the amount of cell killing, and by implication the magnitude of the bystander effect, was significantly greater in the high-density cultures, with an approximately 2.5-fold increase in the amount of cell killing at the highest dose tested. A significant increase in the transformation frequency was also observed at the high density. These data indicate that the magnitude of the bystander effect is dependent on cell density in C3H 10T½ cells, implicating the involvement of gap junction-mediated intercellular communication in transmitting the bystander effect. Several studies have now shown that inhibition of this gap junction activity in cells irradiated in close contact results in decreased levels of the bystander effects for a variety of biological end points. An alternative, but unlikely, explanation is that the observed effect is due to some factor released into the medium, which, because of a very short half-life, can migrate only small distances from the irradiated cell. This is unlikely because it has been estimated that for the irradiation protocol used in the present study, any bystander signal induced could travel over a large distance through the medium during irradiation (approximately 600–700 μm).

The results obtained for low-density cultures did deviate from those expected in the absence of a bystander effect, suggesting that such an effect may still be operative. Considering oncogenic transformation, in the absence of a bystander effect, a transformation frequency of $2.1/10^4$ viable cells is expected that is less (although not significantly) than the observed frequency of 3.3 (Table 1). A similar result was seen for clonogenic survival with a non-significant increase in cell killing (Fig. 1). However, any bystander effect evident in the low-density cultures is likely to result from interaction of a secreted cytotoxic factor with unirradiated cells rather than from direct communication due to the very low frequency of cell-to-cell contact. This has been confirmed in a previous study of low-density cells in which a random distribution of damaged cells throughout the population was seen, suggestive of an extracellular factor.

In conclusion, the present study confirms that when cells are exposed to low doses of α particles, the degree of cell- to-cell contact at the time of irradiation is important in transmission of the bystander signal. When cells are in close contact, gap junctions play a major role, whereas if the degree of contact is low, the bystander effect is mediated by the release of factors into the surrounding environment.

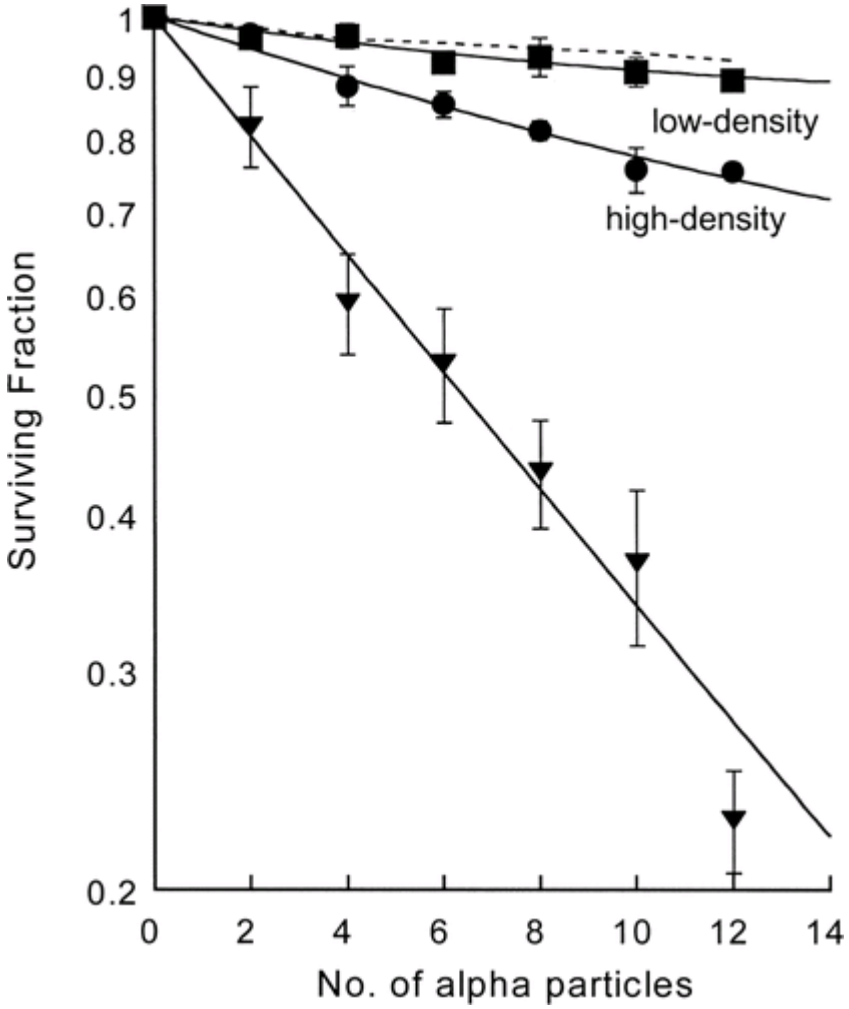

FIG. 1. Clonogenic survival of C3H 10T½ cells after nuclear traversals by 5.3 MeV α particles. Data points represent the means ± SEM from at least three repeat experiments. The triangles indicate survival when all cell nuclei on the dish are exposed to a range of α-particle traversals, from 2 to 12 per nucleus. The dotted line shows the percentage of cells that would be expected to survive when 10% of the cells are irradiated and is calculated from the survival observed when all cells are irradiated. The circles and squares show survival when 10% of the cells are irradiated at high and low density, respectively. The extent to which survival seen at the two densities falls below the dotted line indicates the magnitude of the bystander effect

No. of cells plated, no. of α particles	Clonogenic surviving fraction (plating efficiency) (±SEM)	No. of dishes exposed	No.[a] of viable cells exposed/10^4	No. of transformants produced	Transformation frequency/10^4 surviving cells
200, 0	(0.23 ± 0.02)	71	0.9	1	1.1
2000, 0	(0.17 ± 0.03)	60	2.1	1	0.5
200, 8	0.93 ± 0.02	155	1.8	6	3.3
2000, 8	0.81 ± 0.01	73	1.5	14	9.6

[a] Estimated, accounting for plating efficiency and clonogenic survival.

TABLE 1 Clonogenic Survival Rates, Number of Dishes Exposed, Numbers of Viable Cells Exposed in Transformation Studies, Number of Transformed Clones Produced, and Transformation Frequencies for Microbeam Irradiations

II. Bystander and adaptive response

1. Introduction

Current estimates of cancer risk at low doses (<20 cGy) in the general population are generally derived using the linear, non-threshold (LNT) model which extrapolates to low doses data collected at higher doses from the Japanese atomic-bomb survivors. This model implies a linear relationship between cancer induction and dose in the low-dose region. However, evidence has now emerged for a number of biological phenomena that may be important in determining the cellular response to low doses of radiation. These include the bystander effect, adaptive response, genomic instability and low-dose hyper-radiosensitivity. These phenomena have been predominantly demonstrated with cell lines in vitro but if they were applicable in vivo, they may result in an overall risk which is a nonlinear function of dose. This would have implications for the applicability of the LNT model in extrapolating data into the low-dose region.

The bystander effect is defined as the observation of a biological response in cells that are not themselves traversed by ionizing radiation, but which can communicate with cells that are. This is in contrast to the adaptive response where a low priming dose of radiation (<10 cGy) induces a protective adaptive response often against a high challenge dose.

Both phenomena have been demonstrated for numerous biological endpoints including alteration in gene expression, induction of micronuclei, clonogenic survival and neoplastic transformation. However, the mechanisms by which they operate are still not fully understood. Two main processes are thought to underlie the bystander response depending upon the degree of cell-to-cell contact at the time of irradiation: direct communication between cells involving gap junctions and/or secretion of a cytotoxic factor into the surrounding medium. Any factor transferred through gap junctions would by necessity be small (<2000 Da), whereas the cytotoxic factor(s) secreted into the media is thought to be a protein-like molecule. Considering the adaptive response, it is thought that a low priming radiation dose may enhance DNA repair ability through p53 and cellular antioxidant activity.

Although both the bystander effect (via apoptosis and differentiation) and adaptive response may be protective mechanisms causing overestimation of the low-dose risk by the LNT model, the bystander effect may also increase the risk through the transmission of DNA damage and genomic instability. Consequently, the bystander effect and adaptive response may operate in opposite directions to produce an overall biological effect, but to date there are only limited studies concerning their direct.

The present study used a novel radiation set-up to assess the interaction of these two potentially conflicting phenomena for the endpoints of clonogenic survival and oncogenic transformation.

Both a bystander effect and adaptive response have been shown to be induced via the transfer of supernatant from irradiated cells onto unirradiated cells. In the present study, we set out to confirm whether such effects could be demonstrated in C3H 10T1/2cells.

2. Materials and methods

2.1. Cell culture

C3H 10T1/2cells (passages 9–12, received from Dr J. B. Little, Harvard School of Public Health, MA, USA) were routinely cultured in 75 cm2 tissue culture flasks and grown in minimum essential medium (Eagle modified) (Mediatech Cellgro, Herndon, VA, USA) supplemented with 10% foetal calf serum (Hyclone Laboratories, Inc., South Logan, UT, USA) and penicillin/streptomycin (Gibco-BRL, Life Technologies, Gaithersburg, MD, USA) for all experimental procedures. All cell cultures were incubated at 37°C in humidified 5% CO_2/95% air. All plasticware used in the current study was purchased from Corning, Inc. (Corning, NY, USA).

2.2. Adaptive versus bystander response

The irradiation apparatus employed in this study consists of a metal outer and inner ring, which fit together as shown on the left in figure 1. The rings were designed and manufactured in the Design and Instrument Shop of the Center for Radiological Research. The outer ring (internal diameter 38 mm) has a base of 6 mm mylar (Steinerfilm, Inc., Williams-town, MA, USA) while the inner ring (internal diameter 35 mm) has seven, 2 mm strips of 38 mm mylar on the base. The mylar was fixed to the base of the metal rings using epoxy (EP21LV, Master Bond, Inc., Hackensack, NJ, USA) and baked for 2 h at 150°C until the adhesive was cured. Following sterilization with 70% ethanol, the rings are fitted together such that the mylar strips of the smaller ring sit directly on the mylar base of the larger ring. The cells can then be plated at the desired concentration. In this way, cells attach to both the 6 mm mylar and the top surface of the 38 mm mylar strips. The rings are irradiated from underneath using a track segment facility. The energy of the a-particles (5.3 MeV, stopping power 90 keV/micron) is such that they can penetrate the 6 mm mylar, irradiating cells attached to this layer but are unable to pass through the 38 mm mylar layer. Therefore, cells growing on the strips remain unirradiated but are in close physical proximity to irradiated cells. Following irradiation and further incubation, the rings can then be separated and the bystander cells removed from the strips and studied for several endpoints.

Eighteen hours before irradiation, C3H 10T1/2 cells were plated in 2 ml media at a concentration of 56105 cells per ring and allowed to attach. At this concentration, the cells appeared confluent at the time of irradiation, with the bystander cells on the 38 mm mylar being in physical contact with the cells on the 6 mm mylar. Cells were exposed to either 0 or 2 cGy 250 kVp X-rays at 5 mA with 0.5 mm copper and 1 mm aluminium external filters. The absorbed dose rate was calculated to be 8.5 cGy min^{-1}. Five hours after the initial exposure, cells were either sham irradiated or irradiated with a-particles to a total dose of 5 Gy using the track segment mode of a 4 MeV Van de Graaff accelerator. The effect of irradiating medium alone was also examined to investigate the contribution of factors which may be generated in the irradiated medium. The rings were then returned to the incubator for either 24 or 48 h before assessment of clonogenic survival and oncogenic transformation (24 h only) as described in Section 2.5.

2.3. Adaptive medium transfer

C3H 10T1/2 cells were seeded into a series of 25 cm^2 flasks at an initial density of $5e10^5$ cells per flask and maintained in culture until they reached confluence, usually 24 h. Several flasks were then selected and either sham-irradiated (protocol A) or exposed to a 2 cGy dose of X-rays (protocol B) and returned to the incubator. Eighteen hours following irradiation, the supernatants were removed from these donor cultures and transferred onto unirradiated, confluent cell cultures from which the media had been aspirated. These recipient cell cultures were returned to the incubator for a further 5 h before being exposed to a 4 Gy dose of X-rays (at 15 mA). Following irradiation, cells were either trypsinized and plated immediately (IP) or incubated for a further 24h at 37°C before trypsinization (delayed plating, DP). For comparison, a classic adaptive response protocol was also employed whereby confluent cell cultures were directly irradiated with 2 cGy and challenged 5 h later with 4 Gy (protocol C). Clonogenic survival and oncogenic transformation were assessed as described in Section 2.5.

2.4. Bystander medium transfer

The method employed has been described elsewhere (Mothersill and Seymour 1997). Briefly, 100-mm dishes containing viable cells for assessment of clonogenic survival were set up as detailed in Section 2.5. 150 cm^2 flasks used to generate donor medium were plated with $6e10^5$ C3H 10T1/2 cells and 18 h later these flasks were irradiated with 5 Gy X-rays and returned to the incubator. The medium was then removed from these flasks 18 h after irradiation and filtered through a 0.22 micron filter to ensure that no cells could be present. Medium was removed from the dishes containing cells at cloning density and the filtered medium added. Filtered medium from unirradiated donor flasks was transferred to control dishes at the same time. All dishes were then returned to the incubator to allow for cell growth.

2.5. Cell survival and oncogenic transformation

To assess radiation-induced oncogenic transformation and clonogenic survival, approximately 300 or 100 viable cells were plated into 100 mm dishes respectively. For transformation studies, culture medium was changed at 12 day intervals during the 7-week incubation. The cells were then fixed in formalin, stained with Giemsa and transformed foci types II and III scored as described. Cells plated for clonogenic survival were incubated for 2 weeks without medium change, stained with 2% crystal violet and colonies >50 cells scored.

Data from a minimum of three independent experiments were pooled. All data for clonogenic survival were presented as a mean together with standard error. The statistical significance of differences between groups was tested by Student's t-test.

3. Results

3.1. Adaptive versus bystander response

As shown in figure 2, a significant decrease in surviving fraction from control levels was observed in the non-hit bystander cells following both 24 and 48 h co-culture with cells irradiated with 5 Gy a-particles (24 h: SF=0.77+/-0.01; $p<0.0001$) using the double-ring irradiation apparatus. There was no significant difference in survival between the two time points

studied. However culture of cells with irradiated medium alone had no effect on survival of the non-hit bystander cells at either time point (24 h: SF=1.00+/-0.02). When cells were exposed to a 2cGy priming dose 5 h before being co-cultured with irradiated cells, the majority of the bystander killing was lost and the surviving fraction was not significantly different from control levels at both time points (24 h: SF=0.96+/-0.02).

Table 1 shows the oncogenic transformation frequencies obtained following 24 h of co-culture with irradiated cells. Bystander cells showed a significant increase in transformation frequency over spontaneous control levels ($p<0.0001$). As was observed for clonogenic survival, cells pretreated with the priming dose showed a 2.7-fold significant decrease in transformation frequency from that observed in bystander cells (p,0.0001) to a level that was not significantly different from control levels. Again, no significant increase in transformation frequency was seen following co-culture with irradiated medium only.

3.2. Adaptive medium transfer

The clonogenic survival and transformation results for the adaptive medium transfer assay are shown in tables 2A and B. Pretreatment of cells for 5 h with irradiated-conditioned medium (2 cGy X-rays) before the 4 Gy X-ray challenge dose (protocol B) had no significant effect on clonogenic survival compared

with cells directly irradiated with 4 Gy or those treated with sham-irradiated medium and irradiated with 4 Gy (protocol A). This was true whether the cells were processed immediately after the acute exposure (table 2A) or held in plateau phase for 24 h before trypsinization (table 2B). However, following immediate plating (table 2A), an approximate twofold reduction in the oncogenic transformation frequency was observed in cells treated with irradiated supernatant (protocol B) compared with directly irradiated cells or those treated with sham-irradiated medium (protocol A), although it did not quite reach statistical significance ($p=0.06$). No increase in discrimination was seen when the cells were incubated for 24 h before processing (table 2B). A similar result was seen for both endpoints when cells were directly irradiated with 2 cGy before being exposed to the challenge dose (protocol C).

C3H 10T1/2 cells showed a marked repair of potentially lethal damage for all treatments (table 2B). When they were held in plateau phase for 24 h before processing a significant increase in survival ($p<0.0001$) and an approximate threefold significant reduction in transformation frequency per viable cell was seen for all treatments ($p<0.001$).

3.3. Bystander medium transfer

Figure 3 shows the clonogenic survival obtained when unirradiated cells were treated with either irradiated (5 Gy X-rays) or unirradiated medium taken from cells 18 h post irradiation. Growth in irradiated medium significantly reduced the clonogenic survival of the cells (SF=0.90+/-0.03; pv0.002). Cells treated with medium from unirradiated control flasks had a non-significant increase in survival (SF=1.08+/-0.04).

4. Discussion

Epidemiological studies on the Japanese atomic-bomb survivors provide the best estimate of cancer risk over the dose range 20–250 cGy. The risk of exposure to lower doses of radiation is currently estimated by extrapolating back from the definitive high-dose data using a linear, non-threshold (LNT) model.

There is now a large body of experimental evidence both in vitro and to a lesser extent in vivo for a number of biological phenomena, which may have a role in modulating the shape of the dose– response curve below 20 cGy causing deviation from the LNT model. These phenomena include, but are not limited to, the bystander effect and adaptive response.

To date there are only limited data concerning the direct interaction of the bystander effect and adaptive response. Two of these studies have made use of charged-particle microbeams whose precision is of particular importance for bystander studies as they allow charged particles to be targeted to individual cells within a population. However, although the double-ring irradiation protocol used in the present study cannot offer the same precision, it does offer some advantages over the previous microbeam-based studies. It allows only non-hit cells to be examined, in contrast to the previous studies where both the hit and the bystander cells contributed to the biological outcome. A further advantage is the greater number of cells which can be processed. Although the microbeam has an irradiation throughput of approximately 3000 cells/h, up to 105 bystander cells/ring are available using the track segment protocol, making the experiments less labour intensive.

In the present study, a significant bystander effect was seen for both clonogenic survival and oncogenic transformation in non-hit, bystander cells after 24 h of incubation with targeted cells (table 1). This confirms previous microbeam-based studies where a significant bystander effect was observed for the same endpoints. At the density at which the cells were plated in the current study, the vast majority of cells were in close contact at the time of irradiation. Therefore, it is possible that the irradiated cells could transmit the bystander signal to non-hit cells either through the secretion of a soluble, extracellular factor into the medium and/or through direct cell-to-cell communication via gap junctions. However, no effect on either endpoint was observed when bystander cells were co-cultured in the presence of irradiated medium alone. This is in agreement with previous reports, suggesting that irradiation of medium alone does not produce any cytotoxic factors.

Exposure of bystander cells to a low dose of X-rays (2 cGy) cancels out the majority of the bystander effect generated by high-linear energy transfer a-particles, confirming the findings of previous microbeam-based. In one such study also involving C3H 10T1/2 cells, a 2-cGy priming dose delivered 6 h before a-particle exposure cancelled out about half of the observed bystander effect for clonogenic survival. However, although a decrease in transformation frequency was observed in cells treated with the priming dose in this previous study, it did not reach statistical significance. This may reflect the protocol used as induced cell stress due to immediate trypsinization following the challenge dose may have interfered with the mechanism(s) underlying the adaptive response. In contrast, in the present study the cells were left undisturbed for 24 h following the challenge dose, allowing any adaptive response to be fully expressed.

Previous studies have shown that in comparison with untreated cells, unirradiated bystander fibroblasts treated with the supernatant from cells irradiated with 1 cGy a-particles or c-rays, showed a significant increase in clonogenic survival following subsequent exposure to high or low-linear energy transfer radiation. This is in contrast to the present study where no increase in cell survival was observed (tables 2A and B) although a similar protocol was followed and highlights the cell phenotype specific nature of the adaptive and bystander responses. However, a non-significant ($p=0.06$) 2.4-fold reduction in the transformation frequency was observed in cells treated with irradiated supernatant (protocol B) compared with directly irradiated cells. This suggests that supernatant from cells exposed to 2 cGy X-rays may contain a factor(s) which acts on unirradiated, bystander cells, reducing their susceptibility to oncogenic transformation, but not cell killing.

A significant adaptive response has been demonstrated for oncogenic transformation following chronic exposure of cells to c-rays at doses below 10 cGy. This may be due to selective killing of cells by low-dose hypersensitivity. In the present study a nonsignificant ($p=0.07$) 2.2-fold reduction was seen in the transformation frequency for cells directly irradiated with 2 cGy followed by a 4-Gy challenge dose (protocol C), in agreement with a previously published study. As in the present study, they found no improvement in clonogenic survival and suggested that this may result from different endpoints being dependent upon unique pathways for their expression. Although both the amount of cell killing and transformation frequency were significantly lower following a further 24 h of incubation before processing (table 2B), the discrimination between the protocols was not enhanced by allowing extra time for adaptation as has been observed in other studies.

It is interesting to note that in the present study, cells directly irradiated with a 2-cGy priming dose followed by a subsequent 4 Gy challenge dose (table 2A: protocol C) showed no increase in survival, in contrast to bystander cells in the double-ring experiments which were treated with a priming dose followed by co-culture with irradiated cells and which showed a significant adaptive response for survival (figure 2). Although it may be related to the size of the challenge dose, this suggests that following exposure to a priming dose of X-rays and consequent induction of the adaptive mechanism(s), C3H 10T1/2 cells are less sensitive to the deleterious effects of a bystander signal, but just as susceptible to damage from a direct, high-dose exposure to X-rays.

Medium removed from cells irradiated with 5 Gy X-rays was also able to induce a significant bystander effect in unirradiated cells as shown by an increase in cell killing (figure 3). This has been seen in previous studies and is suggestive of the fact that irradiated cells secrete a cytotoxic factor into the medium which is then able to elicit a bystander effect in unirradiated cells. It was shown to be cell-line specific with keratinocytes, but not fibroblasts, being able to induce the effect. However, the degree of cell killing in the present study was several-fold less than that observed in this previous study, where although using a similar protocol, up to 90% cell killing was seen in keratinocyte cultures as opposed to 10% in the present study. This may be due to the fibroblastic origin of C3H 10T1/2cells and it would be of interest to see if the use of keratinocyte cultures as medium donors would be able to induce greater cell killing in C3H 10T1/2 bystander cells. Control cells, treated with medium from unirradiated cultures showed a non-significant increase in surviving fraction. This may be due to the medium becoming conditioned from the

high-density cultures during the 18 h incubation period and then conferring a survival advantage on the cells to which it is transferred.

Although there are several differences in the protocols used making a direct comparison difficult, the amount of bystander cell killing seen in the medium transfer experiments was twofold less than that seen when using the double-ring protocol (figure 2 versus figure 3). This may be a result of the bystander signal being transmitted between cells via gap junctions in addition to the secretion of a cytotoxic factor into the medium in the high-cell density double-ring protocol. This may lead to a subsequent increase in cell killing confirming the importance of cell-to-cell contact at the time of irradiation in transmitting the bystander response.

In conclusion, the results indicate that the cellular response to radiation is dependent upon the interaction between several competing phenomena, the relative importance of which remains unclear. Although both the bystander effect and the adaptive response have been demonstrated in vivo their relevance at the tissue level is yet to be fully elucidated. Therefore the question of whether it is necessary to revise the LNT model to more accurately reflect the radiation risk at low doses remains unanswered.

Figures and tables can be found in Mitchell S.A., Marino S.A., Brenner D.J. and Hall E.J. Bystander effect and adaptive response in C3H 10T1/2 cells. Int. J. Radiat. Biol. 80:465-472 (2004).

Figure 1. Double-ring apparatus used. The inner ring (internal diameter 35 mm) with 38-mm mylar strips (width 2 mm) is shown on the right with the complete double-ring apparatus on the left (outer ring diameter is 38 mm).

Figure 2. Surviving fraction of bystander C3H 10T1/2 cells co-cultured either with cells (‘bystander’) or culture media (‘media’) irradiated with 5 Gy alpha particles. Results are also shown for bystander cells pretreated with a 2-cGy priming dose 5 h before co-culture with irradiated cells (‘adaptive’). Data were pooled from at least three independent experiments (mean+/-SEM).

Figure 3. Surviving fraction of unirradiated C3H 10TKcells cultured in media from either unirradiated donor cells or cells irradiated with 5 Gy X-rays 18 h before donation. Survival for cells directly irradiated with 5 Gy is also shown. Data were pooled from at least three independent experiments (mean+/-SEM).

Table 1. Clonogenic survival rates, numbers of viable cells exposed in transformation studies, number of transformed clones produced and transformation frequencies for bystander C3H 10T1/2 cells co-cultured for 24 h with cells (‘bystander’) or media (‘media’) exposed to 5 Gy alpha particles. Results are also shown for cells irradiated with a 2-cGy priming dose 5 h before co-culture with irradiated cells (‘adaptive’). Data were pooled from at least three independent

experiments (mean+/-SEM).
*Estimated, accounting for plating efficiency and clonogenic survival.

Table 2A. Clonogenic survival rates, numbers of viable cells exposed in transformation studies, number of transformed clones produced and transformation frequencies for C3H 10T1/2 cells. Cells were either directly exposed to 4 Gy X-rays or: (1) supernatant from sham-irradiated cells (protocol A); (2) supernatant from cells exposed to 2 cGy X-rays (protocol B); or (3) a 2-cGy priming dose (protocol C). Following a further 5 h of incubation at 37°C, these cells were challenged with 4 Gy and processed immediately (IP).

*Estimated, accounting for plating efficiency and clonogenic survival.

Table 2B. Clonogenic survival rates, numbers of viable cells exposed in transformation studies, number of transformed clones produced and transformation frequencies for C3H 10T1/2cells. Cells were either directly exposed to 4 Gy X-rays or: (1) supernatant from sham-irradiated cells (protocol A); (2) supernatant from cells exposed to 2 cGy X-rays (protocol B); or (3) a 2-cGy priming dose (protocol C). Following a further 5 h of incubation at 37°C, these cells were challenged with 4 Gy and incubated for 24 h before processing (DP).

*Estimated, accounting for plating efficiency and clonogenic survival.

III. Preliminary studies: Biological effects in unirradiated human tissue induced by radiation damage up to 1 mm away

A central tenet in our understanding of radiation-induced biological damage has been that the initially affected cells were directly damaged by the radiation, either by the radiation track itself or through consequent nanometer-ranged, short-lived free radicals. By contrast, a range of evidence has now emerged concerning so-called "bystander" responses involving damage to cells that were not directly traversed by ionizing radiation, being located at significant distances from the directly hit cells. Bystander effects were first reported for the endpoint of sister chromatid exchanges; since then, they have been observed for many endpoints, including clonogenic survival, chromosome aberrations, apoptosis, micronuclei, *in vitro* oncogenic transformation, mutation induction, genomic instability, and changes in gene expression. *In vitro*, bystander effects have been observed to be mediated by direct gap-junction signaling as well as by molecules secreted into medium. Such long-range effects are of interest both mechanistically and for assessing the risk from a low-dose exposure to a carcinogen such as ionizing radiation, where only a small proportion of cells are actually directly hit.

Almost all bystander-effect studies to date have been carried out by using conventional single-cell *in vitro* systems that do not have a realistic three-dimensional, multicellular structure. A few studies have been reported in monolayer explants, but no studies have as yet been reported in normal, three-dimensional human tissue. Given that the bystander phenomenon must involve cell-to-cell communication, directly or indirectly, the relevance of single-cell studies is questionable; thus, experimental models that maintain tissue-like intercellular signaling and three-dimensional structure are important to assess the relevance of bystander responses for human health (in particular, to estimate the range of these bystander signals in human tissue). Here, we report bystander responses in a three-dimensional, normal human tissue system; specifically, a reconstructed human skin model is used. This study is made possible by the use of a charged-particle microbeam, which allows irradiation of cells in defined locations in the tissue yet guarantees that cells more than a few micrometers away receive no radiation exposure.

Bystander responses have been reported in single-cell systems for endpoints that might be considered detrimental [such as mutational or chromosomal damage] as well as protective against carcinogenesis [such as cell killing]. Consequently, in this study, we have chosen one endpoint from each category: induction of micronuclei and induction of apoptotic cell death.

Methods

Reconstructed Human Skin Systems. We report bystander responses in two types of reconstructed, normal human three-dimensional skin tissue systems (MatTek, Ashland, MA), shown in Fig. 1. These systems are generated by growing differentiated keratinocyte cultures on acellular or fibroblast-populated dermal substrates. One of the systems reconstructs the human epidermis, and the other is a "full-thickness" skin model corresponding to the epidermis and dermis of normal human skin.

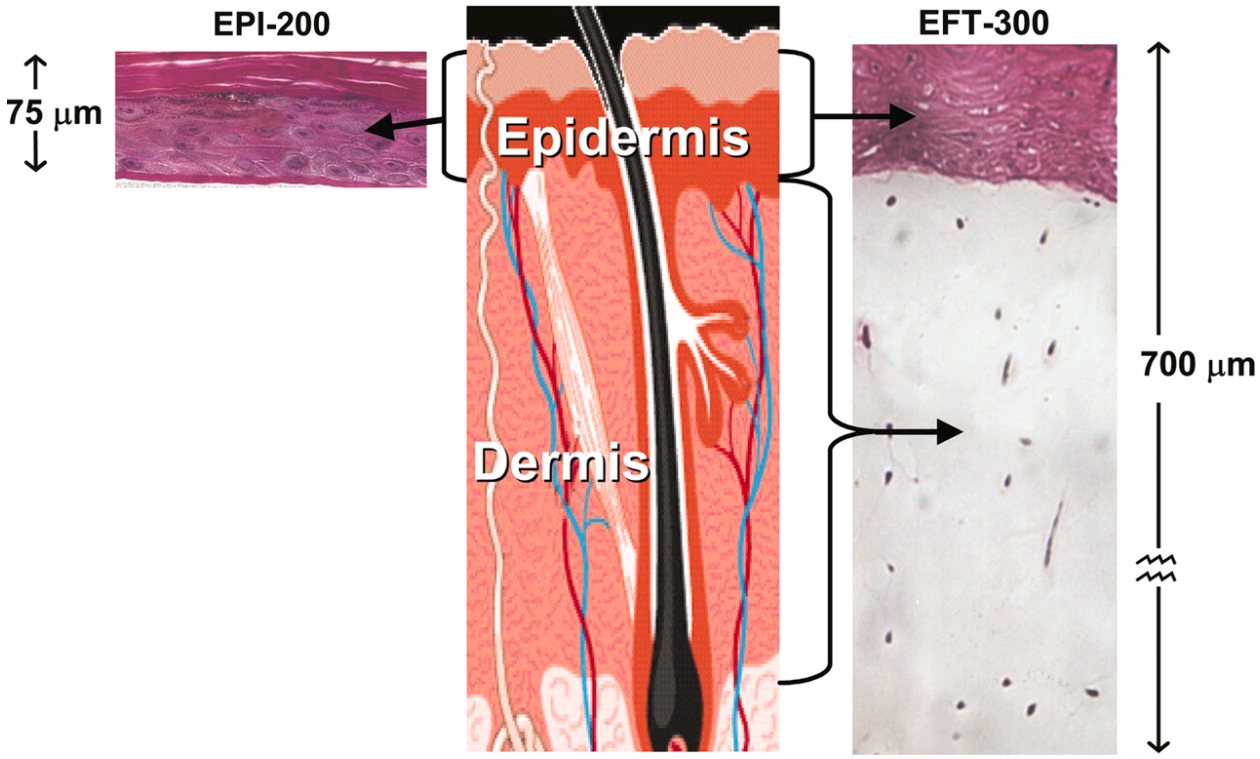

Fig. 1.

The two reconstructed normal human skin tissue systems used here. Shown are the keratinocyte-containing epidermis (EPI-200, *Left*) and full-thickness skin (EFT-300, *Right*), consisting of a dermal layer containing fibroblasts and an epidermal layer similar to that in EPI-200, containing keratinocytes.

Morphologically, these reconstructed tissues show very similar microarchitectures to the corresponding tissue *in vivo*: Epidermal layers of the skin models consist of basal, spinous, granular, and cornified layers, analogous to those found *in vivo*. Analysis of the tissue microstructure has demonstrated the presence of keratohyalin granules, tonofilament bundles, desmosomes, and a multilayered stratum corneum containing intercellular lamellar lipid layers arranged in patterns characteristic of the *in vivo* epidermis. The reconstructed tissues are mitotically and metabolically active, maintaining the same differentiation patterns as those *in vivo*. Markers of mature epidermis-specific differentiation such as profilaggrin, the K1/K10 cytokeratin pair, involucrin, and type I epidermal transglutaminase, are expressed. The reconstructed tissues show lipid profiles similar to the corresponding tissue *in vivo*, release the relevant cytokines, and demonstrate the presence of gap junctions.

These reconstructed tissues are very stable and allow a high degree of experimental reproducibility.

Reconstructed Epidermis. The model of the human epidermis (Fig. 1 *Left*, designated EPI-200) consists of normal human epidermal keratinocytes that have been cultured to form a multilayered, differentiated model of the human epidermis. It closely resembles human

epidermal microarchitecture (see above), with *in vivo*-like morphological and growth characteristics that are uniform and highly reproducible. It contains 8-12 cell layers and is ≈75-μm thick.

Reconstructed Full-Thickness Skin. The model for full-thickness skin (Fig. 1 *Right*, designated EFT-300) contains both an epidermal layer containing keratinocytes and a dermal layer containing fibroblasts and extracellular matrix. These layers correspond to the epidermis and dermis of normal human skin and are cultured from normal human epidermal keratinocytes and dermal fibroblasts. Histological cross sections of this full-thickness tissue demonstrate an "epidermal" layer that is very similar to the EPI-200 model (see above) on top of a fibroblast-containing, collagen matrix dermis-like layer. The overall thickness of this tissue is ≈700 μm.

Tissue Culture. The reconstructed tissues were cultivated by using an air-liquid interface tissue culture technique: The tissue is grown on a semipermeable membrane, fed with serum-free medium from below, and cultivated on Millicell-CM culture inserts (Millipore) by using a 28-μm hydrophilic membrane. The surface of the tissue is exposed to the air, which stimulates differentiation. The diameter of the tissues is 8 mm, and their useful lifetime is 2-3 weeks.

Microbeam Irradiation. To be able to produce direct radiation damage in cells spatially defined locations in the three-dimensional tissue, and guarantee no direct radiation damage to the remainder of the cells in the tissue, the Columbia University charged-particle microbeam was used. The charged-particle microbeam delivers defined numbers of charged particles (in this case, α-particles) with high accuracy to specified locations. The charged particles are focused with a series of electrostatic lenses to a beam diameter of <5 μm. A detailed description of the microbeam is given in ref. In the current experiments, 7.2-MeV α-particles were used (range ~ 60 μm; initial stopping power of 80 keV/μm). As schematized in Fig. 2, each tissue sample was irradiated with the microbeam such that all of the irradiated cells were in a single thin vertical plane, of thickness no more than two cell diameters, which bisects the tissue sample. Because the α-particles scatter very little (<<1 μm) as they pass through the tissue sample, the arrangement guarantees that cells more than a few micrometers away from the plane of irradiated cells will receive a zero radiation dose.

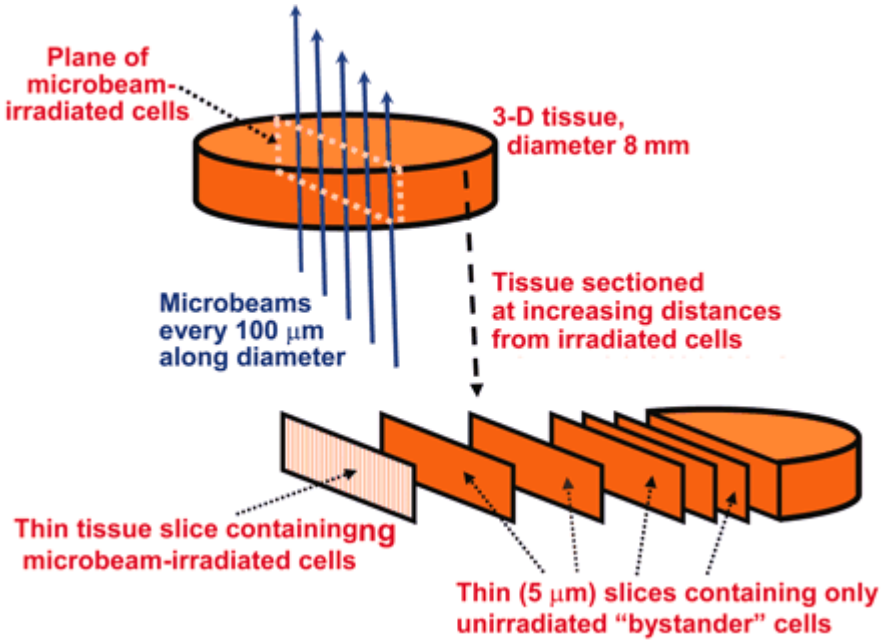

Fig. 2.

Schematic of the irradiation procedure. Each tissue sample consists of an 8-mm-diameter cylinder that is 75 μm (epidermal model, EPI-200) or 700 μm (full-skin model, EFT-300) in height that is microbeam-irradiated along a diameter by α-particles (10 particles every 100 μm along the diameter). The microbeam is <5 μm across, less than one cell diameter, so the plane of irradiated cells is no more than two cells wide. After irradiation, the tissue is fixed and sectioned into 5-μm slices parallel to, and progressively farther from, the irradiated plane of cells.

Irradiation Protocols. The tissue samples were irradiated from below through the membrane that forms the base of the culture insert. The insert was positioned in a custom-designed holder attached to the microbeam stage, with a repositioning accuracy of better than 2 μm. Ten α-particles were delivered every 100 μm along a diameter of each tissue, corresponding to 80 locations across the tissue diameter. Typical total irradiation times were ≈2 min per tissue.

For the EPI-200 epidermal tissue, a given α-particle will traverse 5-10 cells as it penetrates the tissue; thus, as 80 locations across a diameter of tissue were microbeam-irradiated, a total of 400-800 cells located in the designated irradiation plane were actually traversed by α-particles, with each traversed cell receiving an average dose of ≈1 Gy.

For the full-thickness skin (EFT-300) experiments, separate protocols were used to irradiate the tissue from the dermal and the epidermal sides. Thus, one protocol directly targeted only keratinocytes in the epidermis, and the other directly targeted only fibroblast cells (and extracellular matrix) in the dermis. In each case, the keratinocyte cells in the epidermal layer were subsequently assayed for apoptotic cell frequency as a function of the distance from the irradiated plane. No assays were undertaken in dermal fibroblasts because of their low density.

Distance-Dependent Assays. After microbeam irradiation of a single plane across the tissue diameter, each tissue was returned to a multiwell dish filled with fresh medium and incubated at

37°C in a humidified atmosphere with 5% CO_2. At 72 h postirradiation, the tissues were formalin-fixed, paraffin-embedded, and sectioned into 5-μm-thick strips parallel to the plane of irradiated cells (see Fig. 2). As illustrated in Fig. 2, this protocol allows separate analysis of slices of tissue containing only nonirradiated cells, each slice having been located at increasing and known distances from the plane of irradiated cells.

An estimate of the shrinkage produced in the fixed, embedded samples was made by comparing morphometric data obtained with unfixed vs. fixed samples. Shrinkage of ≈10% in each direction was observed, as described elsewhere.

Distance-Dependent Apoptosis Assay. Apoptotic cells were scored in each section on day 3 postirradiation by using a TUNEL enzymatic *in situ* labeling kit (DermaTACS, Trevigen, Gaithersburg, MD) optimized for paraffin sections. This time was chosen based on preliminary experiments to reflect the maximal apoptotic response. Some typical images are shown in Fig. 3. The fractions of apoptotic cells were assessed in 5-μm-thick tissue slices at distances from 200 to 1,100 μm from the plane of irradiated cells and compared with corresponding controls for which the central plane of cells had been sham-irradiated. At each distance, a total of ≈10,000 cells were scored in three repeat samples.

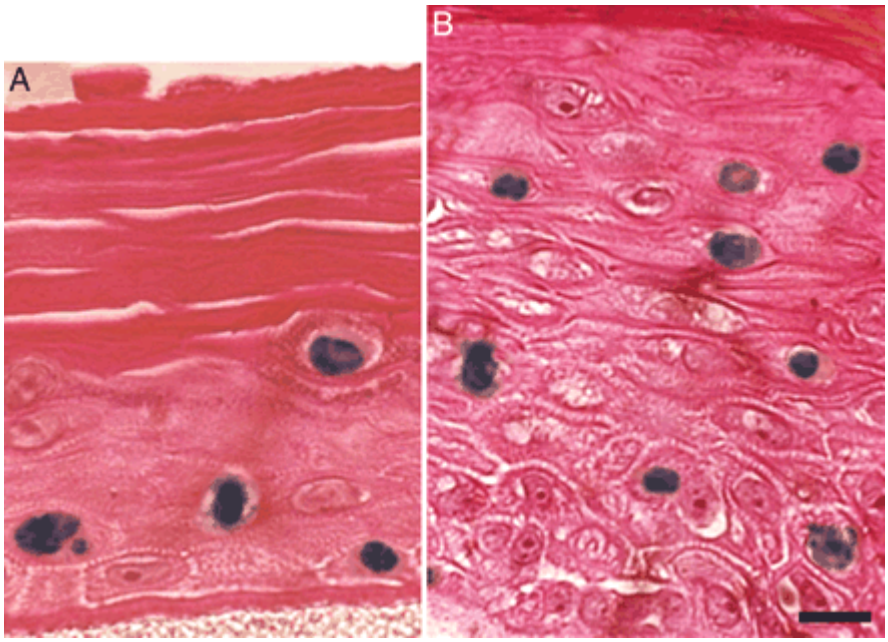

Fig. 3.

Examples of apoptosis in unirradiated bystander cells in artificial human skin systems. Shown are EPI-200 (*A*) and EFT-300 (*B*) stained with a DermaTACS apoptosis kit; positive apoptotic cells appear blue. Each slice of tissue shown was >200 μm from the plane of irradiated cells and thus received no direct or scattered radiation exposure. Formalin-fixed, paraffin-embedded, 5-μm-thick histological sections are shown. (Scale bar: 10 μm.)

Distance-Dependent Micronucleus Assay. Three days were allowed postirradiation for cell proliferation and division to continue. Tissues were then fixed in formalin and paraffin-

embedded, and 5-μm sections were sliced at 100-μm intervals parallel to the plane of microbeam irradiation (different slices thus having been at increasing distances from the irradiated cells). The tissue sections on microscope slides were stained with DAPI, a fluorescent DNA-binding dye that labels all cell nuclei and micronuclei.

Micronuclei and/or nucleoplasmic bridges will result from aberrant mitotic divisions involving chromosomal aberrations. Such events, examples of which are shown in Fig. 4, are readily induced by ionizing radiation and have been seen, *in vitro*, in cells that were known bystanders of known irradiated cells. Frequencies of cell nuclei with associated micronuclei, relative to all nuclei, were recorded in three 500-cell samples at each plane at different distances (200-1,100 μm) from the plane of irradiated tissue, as well as the sham-irradiated control tissues.

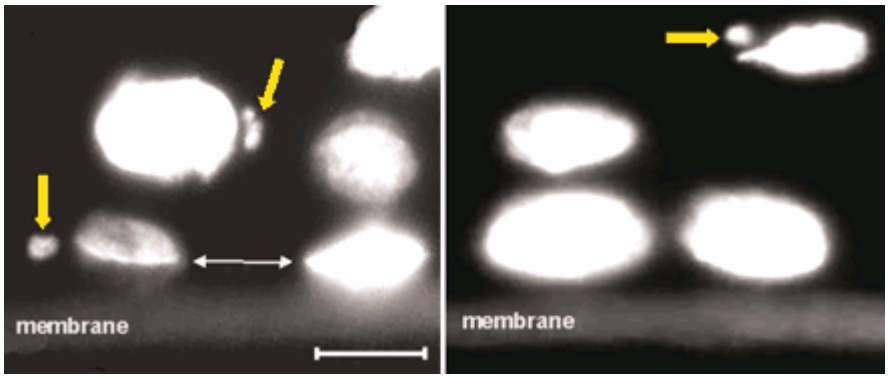

Fig. 4.

Micronuclei observed in unirradiated bystander cells in three-dimensional epidermal tissue (EPI-200) stained with DAPI. Each slice of tissue shown was >200 μm from the irradiated cells and thus received no direct or scattered radiation exposure. The support membrane can be seen at the bottom of each image. The large arrows indicate micronuclei associated with individual cell nuclei. The small arrows show the location of a broken nucleoplasmic bridge, indicating, as expected, a plane of cellular division parallel to the membrane. (Scale bar: 10 μm.)

Controls. The control tissues were handled in exactly the same manner as the irradiated samples, except that the central plane of cells (Fig. 2) was sham-irradiated (i.e., the microbeam was not turned on, so no cells were irradiated).

Statistical Analyses. For the control cells (those in the same location at which bystander responses were probed, but for sham-irradiated tissue samples), to see whether the location of the sample within the tissue was significant apart from any bystander effects, a standard Poisson homogeneity test was performed, intercomparing the results from each slice.

For the nonirradiated cells in the irradiated tissue, we compared the results by using Fisher's exact test, both with the control sample from the same location and, when appropriate (see homogeneity test, above), with the pooled controls from all locations.

Results

For the epidermal skin tissue (EPI-200), Fig. 5 shows the measured fractions of apoptotic cells and micronucleated cells. All of the data shown are for unirradiated tissue, plotted as a function of distance from the irradiated cells or (for the controls) the sham-irradiated cells.

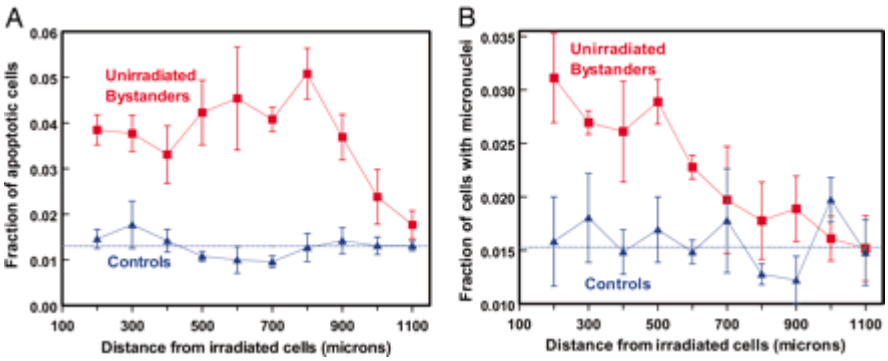

Fig. 5.

Fraction of apoptotic (*A*) and micronucleated (*B*) cells in unirradiated bystander cells at different distances from the plane of irradiated cells in a three-dimensional human epidermal skin model (EPI-200). Controls refer to sham irradiations, with conditions otherwise identical. Dotted lines show mean value of control points. Each data point (and SEM) is derived from experiments with three independent tissues.

For the control cells (those in the same location at which bystander responses were probed, but from sham-irradiated tissue samples), the results for both endpoints were independent of the location within the tissue ($P > 0.25$ using an exact homogeneity test).

For the apoptotic endpoint, a statistically significant bystander response in unirradiated cells relative to the controls was observed at all distances up to 1,000 μm (1 mm) away from the irradiated cells ($P < 0.05$ at each distance, Fisher's exact test, two-sided). Averaged over distances from 200 to 1,000 mm from the plane of the irradiated cells, the mean proportion of apoptotic cells was 3.7 ± 0.6% in the bystander cells vs. 1.3 ± 0.3% in the controls. The bystander-related enhancement in effect over controls was a factor of 2.6 ± 0.4 at a distance of 200 μm from the irradiated cells, and the corresponding enhancement, averaged over all distances from 200 to 1,000 μm, was a factor of 2.8 ± 0.3.

For micronucleus induction, a statistically significant bystander response, relative to the controls, is apparent in unirradiated cells at all distances up to 600 μm (0.6 mm) away from the irradiated cells ($P < 0.05$ at each distance, Fisher's exact test, two-sided). The bystander-related enhancement in effect relative to controls was a factor of 2.0 ± 0.4 at a distance of 200 μm from the irradiated cells, and the corresponding enhancement, averaged over all distances from 200 to 600 μm, was a factor of 1.7 ± 0.3.

Fig. 6 shows the results with the full-thickness skin model (EFT-300), which contains an epidermal keratinocyte layer on one side and a fibroblast-containing dermal layer on the other. Separate protocols were used to irradiate the full-thickness tissue from the epidermal side and the dermal side, each with α-particles of range ~ 60 μm; thus, one protocol irradiates only a plane of epidermal keratinocytes, and the other irradiates only a plane of dermal fibroblasts (plus

extracellular matrix) within the 700-μm-thick tissue. The fraction of apoptotic cells in the keratinocytes in the epidermal layer was assessed as above in unirradiated tissue sections that were at increasing distances from the plane of the irradiated cells.

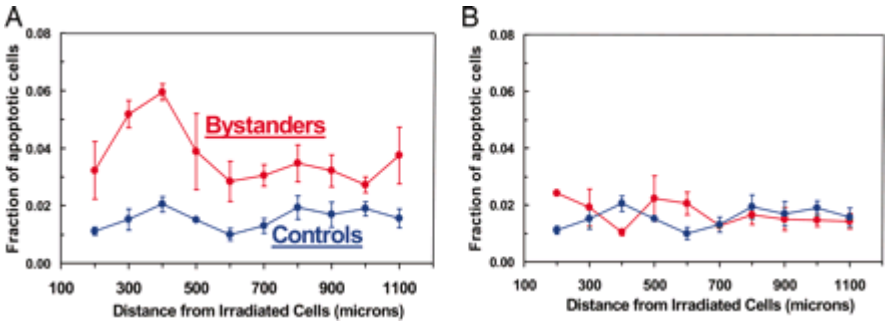

Fig. 6.

Fraction of apoptotic cells in unirradiated keratinocyte layers at different distances from a plane of irradiated cells in a three-dimensional, full-thickness human skin model (EFT-300). Controls refer to sham irradiations, with conditions otherwise identical. Each data point (and SEM) is derived from studies with three independent tissues. (*A*) Microbeam irradiation of a plane of cells only in the epidermal layer, showing a significant bystander response. (*B*) Microbeam irradiation of a plane of cells only in the dermal layer, showing no evidence of a bystander response in the unirradiated epidermal layer.

When the epidermal layer in the full-thickness tissue was irradiated (Fig. 6*A*), there was a clear bystander response extending to 1,100 μm ($P < 0.05$ at each distance, Fisher's exact test, two-sided); this response was very similar to that when the epidermis-only system (EPI-200) was studied (Fig. 5*A*). However, when only the dermal region containing fibroblasts (and extracellular matrix) was irradiated, no bystander response was seen in the keratinocytes (Fig. 6*B*). This observation may suggest that there is no signaling from the dermal to the epidermal layers in terms of the bystander response, although it could simply be the consequence of the distance (≥600 μm) between the irradiated dermal cells and the probed unirradiated keratinocytes.

Discussion

In summary, we have shown that unirradiated human cells in normal, three-dimensional human tissue systems can respond to radiation-induced cellular damage that occurs in cells at quite large distances away. Specifically, the results suggest that the bystander response is propagated over distances up to 1 mm in normal human tissue. We have demonstrated this effect both for a cytogenetic damage endpoint (at distances up to 0.6 mm), which might be expected to be associated with deleterious consequences, and a cell-killing endpoint (at distances up to 1 mm), which, through the elimination of damaged cells, could be associated with protective consequences. Bystander responses for both potentially protective and potentially deleterious endpoints have also been reported in *in vitro* single-cell experimental systems.

The magnitude of the bystander response was clearly statistically significant for both the apoptotic and the micronucleus endpoints, although the magnitude of the response is clearly less

than for directly hit cells. For example, based on *in vitro* results, the frequency of micronucleated cells among those cells that were directly hit by α-particles (based on a dose of ~1 Gy to these hit cells) would be ≈0.25, compared with a maximum frequency of micronucleated cells that we observed among unirradiated bystander cells of 0.03. In contrast, given a bystander-signal range of up to 1 mm, in most low-dose situations, there will be far more potential bystander cells than hit cells.

The shape of the curves in Fig. 3 (relatively flat over a distance of several hundred micrometers) suggests, as have much other data from single-cell systems, that bystander effects are characterized by a binary threshold response (i.e., unirradiated cells respond in a binary way to a damage signal, as long as the intensity of the signal remains above a threshold value). The range of the bystander signal in tissue, up to 1 mm, corresponds to ≈50-75 cell diameters. This surprisingly long range implies either that directly damaged cells produce long-range, diffusible bystander signals, perhaps through autocrine/paracrine mechanisms, or that a cell relay system is active, in which cells signal only their immediate neighbors (juxtacrine signaling), the signal being relayed by spatially intermediate, unirradiated bystander cells.

In terms of potential consequences, bystander responses have been hypothesized to be significant both for radiotherapy, essentially extending the margins of the treatment volume, and for low-dose radiation protection, essentially increasing the number of cells affected by a low radiation dose.

In the radiotherapy context, even a bystander signal range as large as 1 mm would suggest that the bystander effect is unlikely to be a confounding factor at the margins of a radiotherapy treatment volume in the context of the larger uncertainties due to setup variations and organ motion.

By contrast, in the context of low-dose radiation risk assessment, an effective bystander signal range of ≈1 mm would imply that far more cells could be affected by a very low dose of radiation than expected based on simple target theory. Thus, bystander responses may potentially play a significant role in the extrapolation of radiation risks in humans from high doses to very low doses where nonhit bystander cells will predominate; simple extrapolations based on the number of cells directly hit may well be inadequate. At this point, it is not known whether a single α-particle can initiate the types of effects observed here in three-dimensional tissue: In single-cell studies, single α-particles have been reported to induce bystander effects for some endpoints but not for others.

IV. Development of a method for assessing non-targeted radiation damage in an artificial 3D human skin system

Introduction.

Non-targeted radiation effects, where DNA damage induced as a direct consequence of the ionization tracks does not appear to play a fundamental role, occupies a primary role in modern radiobiological studies. Among them, the radiation-induced bystander effect is very well documented and has been widely investigated for different biological end-points in a variety of *in vitro* cell lines. It refers to effects detected in cells that where not directly exposed to ionizing radiation but that have at some stage either shared medium with or being in contact with directed irradiated samples. Despite the fact that the underlying mechanisms are still not well understood, strong evidence has been accumulated suggesting a critical role played by gap-junction inter-cell communication as well as soluble factors released by the directly exposed samples such as cytokines reactive oxygen species (ROS) and nitric oxide (NO). The effects reported are generally dose independent and despite being significantly smaller than those induced by direct radiation exposure they may be of critical relevance in low-dose and/or non-uniform irradiation conditions. Such conditions are likely to arise in medical diagnostic/treatment or even common environment circumstances where the direct radiation damage component is expected to be very small. Moreover, the existence of the bystander effect poses a major challenge to DNA centred theories such as the target theory and the linear no-threshold hypothesis and seems to indicate the requirement of a paradigm shift in radiation biology. The new paradigms may have to take into consideration cell-to-cell and cell-to-matrix signalling to include effects measured in cells not directly "hit" by the radiation. Target sizes larger than the single cell itself and interactions over long distances and times will have to be considered as critical parameters as the absorbed dose. Therefore, the importance of the bystander effect in radiation protection and radiation therapy will have to be evaluated in a new multidimensional context.

In order to evaluate the significance of the bystander effect in terms of risk assessment to patients or regulation of the exposure level, *in vitro* results have to be validated in more complex biological systems that better represent *in vivo* models. The main issue in assessing the bystander response in *in vivo* models is the presence of other systematic factors that may mask the effect making it impossible to attribute a specific phenotype found in unirradiated cells to the signal generated by directly exposed cells. Previous studies addressing this problem have used explant models and *in vitro* tissue equivalents. Monolayer or two dimensional explant models are of limited usefulness as they don't present the full tissue structure and/or differentiation pattern offering only limited cell-cell interaction. On the other hand, tissue models that better resemble *in vivo* cell environments and interactions, present technical challenges for investigating effects such as genomic instability. In order to accurately measure the contribution of the bystander effect to low dose/partial irradiation of tissues, the samples will have to be disaggregated into individual cells that may also be further cultured, while still preserving their spatial correlation. Here, we report the bystander response in a 3-dimentional *in vitro* skin model partially exposed to 3.5 MeV protons. Although the model has been previously used to assess bystander response following microbeam irradiation, in this manuscript we present the development of a new experimental procedure for an *in vivo*-like assay to measure complex radiation damage, such as chromosomal aberrations and mutations where individual cell analysis is required, as a function of their relative position in the tissue. The study presented in this manuscript focuses on the

investigation of micronuclei production to establish the protocol working principle and compare the findings with existing data while providing further insight into the relevance of the bystander effect in 3D biological samples.

2. **Materials and methods**

2.1 Tissue constructs.

The experiments reported in this manuscript were performed using the EPI-200 tissue from MatTek Corporation. The EPI-200 construct is a multilayered (8-12 cell layers, ~75 μm thick), differentiated tissue consisting of basal, spinous, granular and cornified layers with very similar microarchitectures to the corresponding tissue *in vivo*. The EPI-200 tissue also exhibits mitotic and metabolic activity, markers of specific differentiation and presence of gap junction; characteristics of the *in vivo* epidermis. The tissue resembles the human epidermis as it is constructed from normal epidermal keratonocytes (foreskin-derived) and cultured on chemically modified, collagen-coated, 9 mm diameter culture insert (MilliCell CM with 50 μm thick porous membrane). Differentiation is induced by the air-medium gap by keeping the cell insert sitting just on top of the medium surface with the apical surface of the tissue exposed to the environment. The tissues were generally shipped overnight on Mondays and received on Tuesday mornings in 24-well trays. On arrival, the samples were placed in 6-well culture plates, each containing 1 ml of fresh, warmed New Maintenance Medium (NMM). The New Maintenance Medium was provided by MatTek Corporation and it is based on the Dulbecco's Modified Eagle's Medium (DMEM) with addition of keratonocytes growth factors (exact composition is proprietary of the manufacturer). The tissues were incubated at 5% CO_2 and 37^{o}C for approximately 24 h before any experimental procedures took place.

2.2 Irradiation.

Tissue irradiation was performed using the RARAF track-segment facility where a beam of 3.5 MeV protons emerges vertically through a thin metal foil. The samples were irradiated from below (i.e. through the supporting membrane and from the dividing keratonocytes side). The tissue inserts were positioned in a custom-designed holder attached to a rotating wheel through which the samples can be scanned across the radiation beam. During the irradiation (~1 min/sample), the tissues were completely exposed to air. Dehydration was prevented by the supporting membrane being wet and by covering the tissue insert. No sign of dehydration was observed following the irradiation. In order to produce a spatially confined radiation exposure, a 100 μm thick platinum disk with a 50 μm wide slot across it, was placed directly below the tissue supporting membrane. The slot was aligned with the tissue insert so to assure that only a narrow strip of the sample along its diameter was directly exposed to radiation. The portion of the tissue directly exposed to radiation was identified by marking the area of the supporting membrane corresponding to the slot on the platinum disk. Because of the little scattering of the 3.5 MeV protons as they pass through the platinum mask, the supporting membrane and the tissue (± 15 μm as shown by TRIM simulation), the arrangement described above guarantees that cells more than a few tens of microns away from the irradiation area will receive no radiation dose. As the range of 3.5 MeV protons in tissue is around 190 μm, all layers of the portion of the tissue directly exposed will accumulate radiation dose. However due to the loss of energy of the protons as they pass through the sample, the top layer of cell will receive a dose higher (~20 %) than that absorbed by the first layers, proportional to the change in LET ($LET_{entrance}$ = 10.7

keV/µm; LET_{exit} = 12.9 keV/µm). The dose reported in this manuscript refers to the dose absorbed by the cell in the first layers of the tissue sample.

2.3 Tissue slicing and cell harvesting.

Following the irradiation, the tissue samples were immediately incubated in 6 multiwell plates in 2 ml of NMM containing either 1, 3 or 5 µg/ml Cytochalasin B for 24, 48 or 72 hrs. As from technical communication from MatTek Corporation, the tissues could be kept in NMM for up to 5-7 days without significant alteration of their dividing and differentiating process.

For the tissue slicing, the samples were removed from the culture insert by cutting the supporting membrane off. This was done by carefully using a scalpel and a pair for forceps and avoiding any contact with the tissue itself. The tissue-membrane were then sliced using a customer designed microtome. The microtome (shown in figure 1) was designed and realised by the Center for Radiological Research workshop specifically for such application.

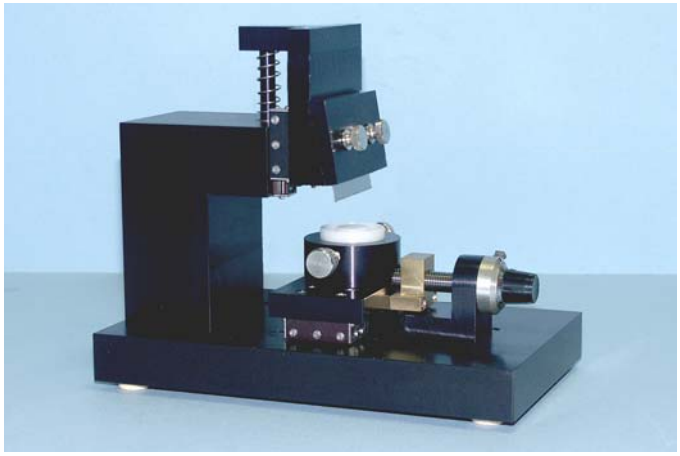

Figure 1. Customer designed microtome used for the tissue slicing.

It basically consists of a vertically sliding razor blade that can be manually pressed against the tissue placed on a micrometer controlled platform. The tissues are placed face-up on the platform (which can accurately rotate to align the irradiated part of the sample with the blade) with surface tension between the plastic platform and the tissue supporting membrane enough to prevent sample movements during the slicing process. The slice width is controlled by adjusting the platform position under the blade using a micrometer orthogonally orientated with respect to the blade. The EpiDerm tissue could be easily sliced down to 50 µm wide strips although the tissues have been cut to a minimum of 200 µm wide slices in the experiments reported in this manuscript to obtain a suitable number of cells/slice for the micronuclei study. By exerting the right pressure on the blade, it is possible to cut only the tissue while keeping the supporting membrane (which is harder to cut) intact. The tissue slices can then be easily peeled off the membrane by using a pair of forceps and under microscope view (x10). During the tissue slicing and peeling off the membrane, the samples are kept moisturized by a small drop (~50 µl) of NMM. For the work described in this manuscript, the Cytochalasin B treatment precedes the

tissue slicing; however, the two operations can easily be inverted in case it is desirable to keep different part of the tissue isolated immediately after the radiation exposure.

Cells from each individual tissue slice were isolated and further processed using the following protocol:

1) each slice is gently washed in PBS and then submerged in a 1 ml epperdorf containing 200 µl of trypsin EDTA (0.1%) and incubated for 30 minutes with frequent shaking.
2) 0.5 ml of DMEM with 10% serum added to neutralize the trypsin action.
3) The cells are then gently centrifuged for 10' @2000rpm
4) After the centrifugation, the supernatant was carefully removed and the cell pellet loosened with gentle agitation in 1 ml of fixative (3:1 methanol: acetic acid, cold and freshly prepared).
5) Cells were incubated at 4^{o}C for 20'
6) The cell suspension was then centrifuged again (10' @2000rpm) and the supernatant discarded.
7) The pellet was finally loosed in a fresh drop of fixative (~20 µl) and then gently pipetted onto a dry microscope slide. One slide was prepared for each tissue slice.
8) The glass slide was left to dry at room temperature for several minutes.
9) Slides were then rinsed in PBS and allowed to dry before being stained with Acridine Orange.

2.4 Micronuclei scoring.

For the micronuclei scoring, cells were stained using Acridine Orange (Sigma) at a final concentration of 0.25 mg/ml in phosphate-buffered saline (PBS) solution for 10 minutes at room temperature in the dark. The slides were sub-sequentially washed with PBS, let dry and assembled with a cover slip using VECTASHIELD Mounting Medium with DAPI (1.5 µg/ml). A minimum of 900 cells per sample were scored in order to determine the fraction of binucleated cells and the percentage of binucleated cells with micronuclei. The Fenech criteria (Fenech, 2000) was used to identify micronuclei.

3. **Results**

3.1 Tissue dissociation.

The enzymatic dissociation treatment described in paragraph 2.3 was derived by optimizing personal communication with the MatTek Corporation and using existing dissociation protocols reported in literature. The procedure is relatively quick (less than 1.5 h per sample) while supplying a very high number of individual cells suitable for a variety of radiation damage assays. Overall, the average number of individual cells obtained was ~2.5x10^{5} cells/sample with more than 90 % viable as by trypan blue exclusion test. The number of cells extracted was in excellent agreement with the number of cells composing the tissue as suggested by MatTek Corporation. Microscopic analysis of the small "pad" of tissue remaining at the end of the enzymatic dissociation also supported such conclusion. The "pad" was generally consisting of only the stratum corneum with occasionally keratonocytes observed. This suggested that we were able to collect almost all cells of interest from the tissue sample with a high level of integrity as required for the determination of radiation damage.

3.2 Cytochalasin-B treatment.

Preliminary experiments were conducted to determine whatever the cell division rate in the tissue was sufficiently high to provide a reasonable number of binucleated cells for the micronuclei assessment. This was determined by incubating the EpiDerm tissue in NMM containing Cytochalasin B at different concentrations for different incubation periods. The data was also used to establish the optimum Cytochalasin B conditions to use for the irradiation experiments. In our study, we follow the formation of binucleated cells up to a period of 72 h (i.e. about 3 average keratinocytes cell cycles) following exposure to three different concentrations of Cytochalasin B (i.e. 2, 3 and 5 μg/ml). As shown in figure 2, incubation time and Cytochalasin B concentration both seems to increase the number of observed binucleated cells. Specifically, at a concentration of 2 μg/ml we observed a roughly linear increase of binucleated cells from ~10% at 24h to nearly 50% after 72h. For the 3 μg/ml, the Cytochalasin B treatment induced about 30% of binucleated cells at 24h which increased to reach a plateau at ~60% at 48h and 72h. Results not statistically different were obtained using a 5 μg/ml concentration (i.e. ~40% binucleated cells at 24h, 55% at 48h and 61% after 72h).

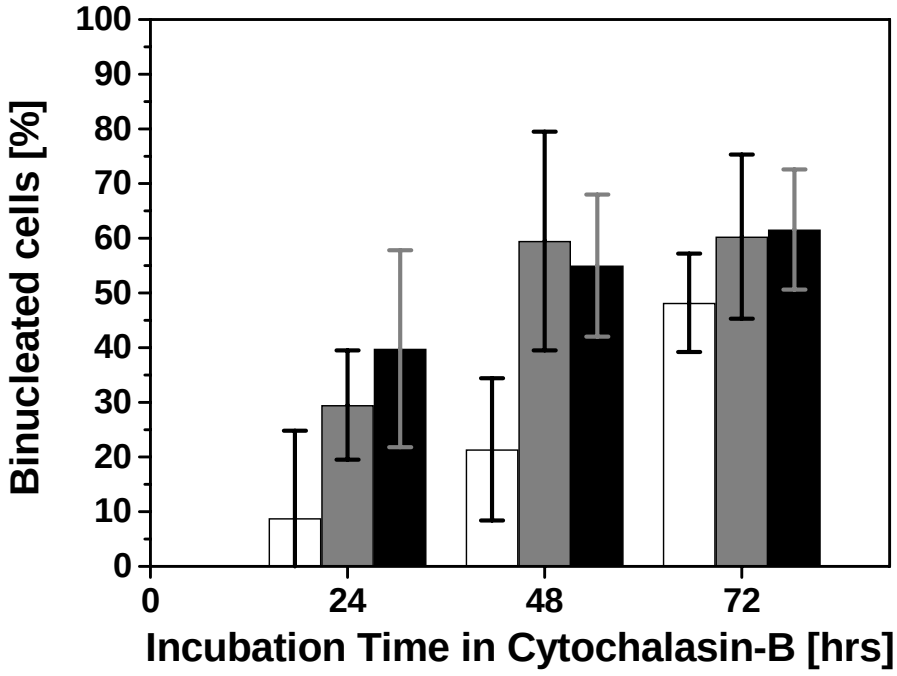

Figure 2. Induction of binucleated cells in EpiDerm tissue due to Cytochalasin B treatment. Concentration of 2 μg/ml (open bars), 3 μg/ml (gray bars) and 5 μg/ml (solid bars).

Although lower than what generally achieved in monolayer cell-culture models (i.e. 70-80%), the data clearly showed that a reproducible and reasonable number of binucleated cells can be obtained with the described protocol. Such number of cells is adequate for the analysis of micronuclei formation as well as a variety of other radiobiological end points. A final concentration of 3 μg/ml for 48h was chosen as standard concentration for the irradiation experiments.

3.3 Bystander micronuclei induction.

Determining the background response level is of critical relevance for the development of a new experimental protocol. In order to have a sensitive and robust model to accurately measure the small effects caused by bystander signal and low dose exposure, it is necessary to have a low and reproducible background response. The micronuclei level measured in the control samples is shown in figure 3 where the fraction of binucleated cells with micronuclei is reported for each stripe the samples have been sliced into. The data indicate an average level of 0.72 ± 0.37 % micronucleated cells. Such level is constant across the whole tissue and sufficiently low to conclude that no significant stress is induced by the above described protocol making it possible to measure small radiation responses. The effect of the stress induced by the slicing procedure has also been assessed by comparing the micronuclei level measured in the unsliced samples with those present in samples with multiple cuts. As shown, there is no statistical difference between the micronuclei level measured as a function of the number of stripes the tissues have been cut into.

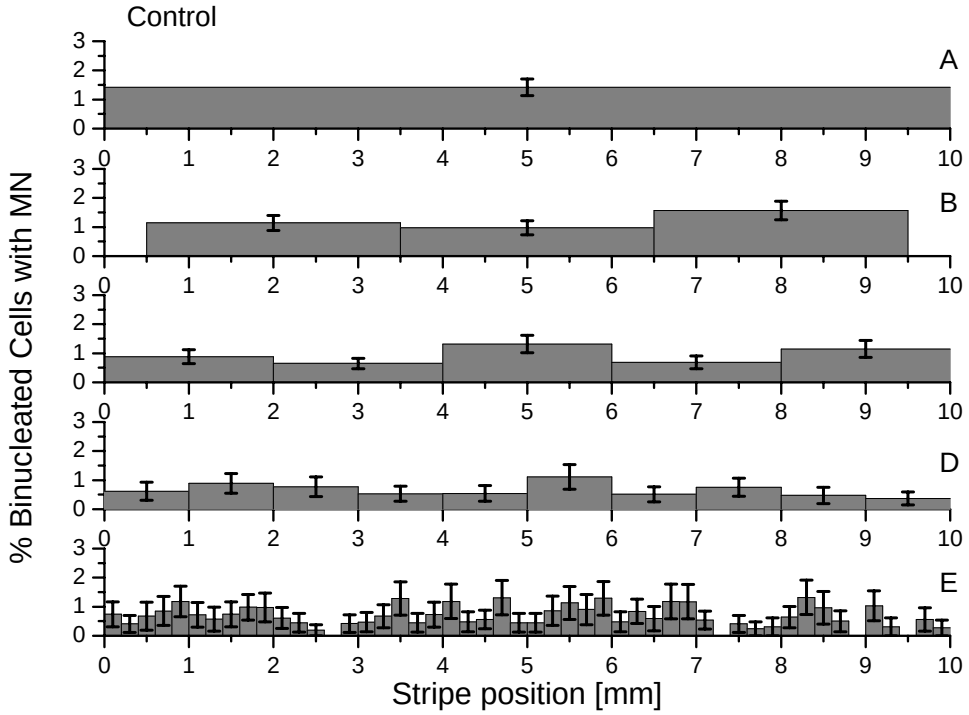

Figure 3. Frequency of micronuclei in unirradiated samples. Panel A, tissues were disaggregated into single cells without being sliced. Panel B, C, D and E, tissues were respectively sliced into 3 mm, 2 mm, 1 mm and 0.2 mm wide stripes before being individually disaggregated. The average frequency measured in our system is 0.72 ± 0.37 % micronucleated cells.

Following a shielded irradiation (50 μm wide line across the tissue diameter) with 3.5 MeV protons, the bystander response has been evaluated by measuring the fraction of cells with micronuclei in each individual stripe the tissues were sliced into. The results are reported as a function of the stripe position relative to the irradiation line for 3 different dose points (0.1, 0.5 and 1 Gy). As reported for the controls, the effect of slicing the samples into different stripe sizes has also been investigated by grouping the data as a function of the number of stripes cut from

each tissue (Figure 4). On average, more than 2000 cells per stripe were scored with the exception of the 0.5 mm stripes where only ~1000 cells were analyzed due to the lower number of cells recovered.

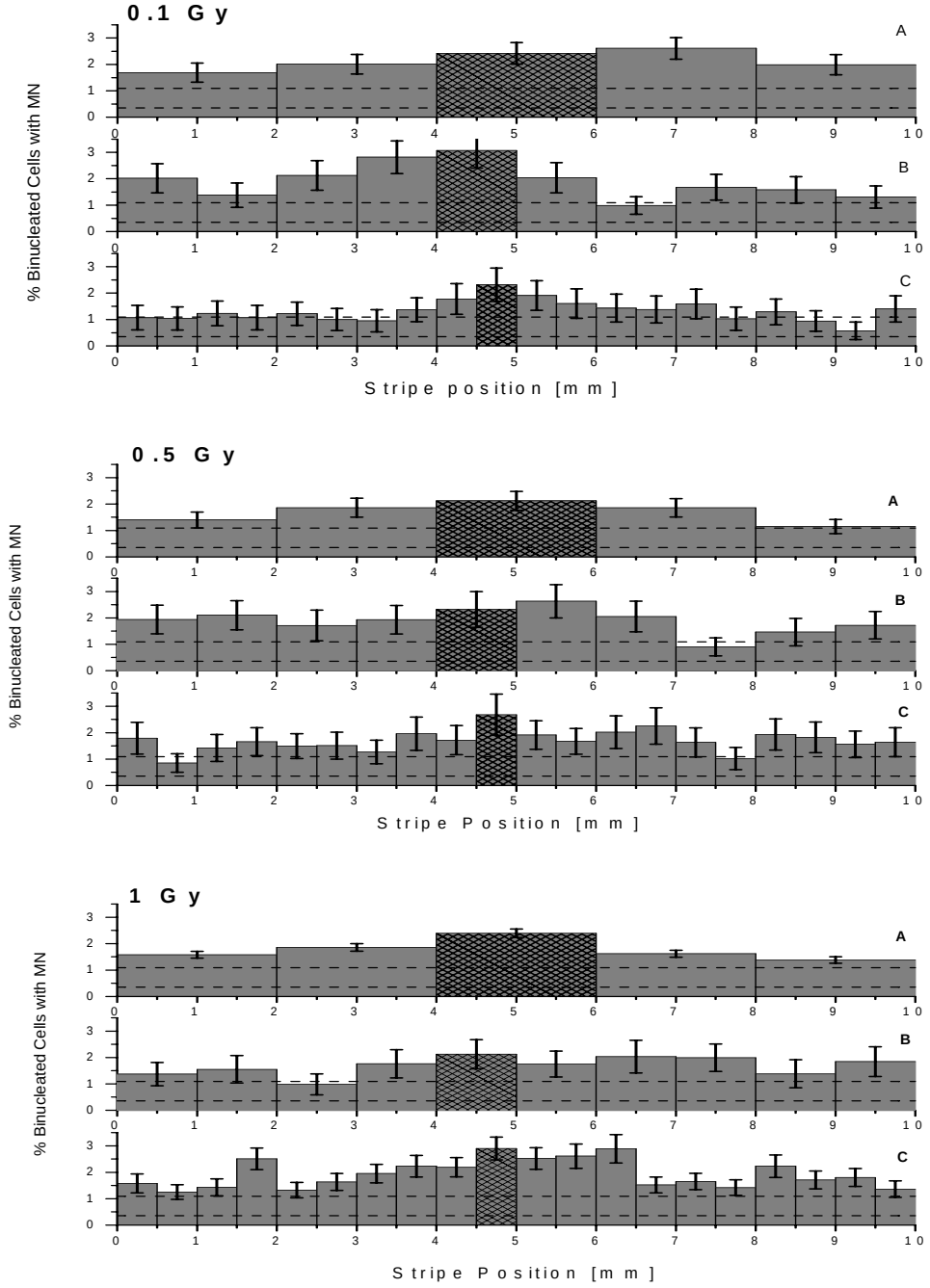

Figure 4. Frequency of micronuclei in irradiated samples (0.1, 0.5 and 1 Gy from top to bottom). Tissues sliced into 2 mm wide stripes are reported in panels A while data relative to 1 mm and 0.5 mm wide stripes are shown on panels B and C respectively. The stripes containing the directly irradiated cells are highlighted. The level of background micronuclei as measured in the control samples (0.72 ± 0.37 % micronucleated cells) is also shown (dashed lines).

A significant increase in the micronuclei formation was measured in almost all irradiated tissues with the maximum occurring in the stripes containing the directly irradiated cells (2.5 - 3.0 % micronucleated cells). Elevated micronuclei percentage was also evident in bystander stripes although the increase relative to the background wasn't always statistically significant. Interestingly, while clear differences from the controls have been measured in the tissue samples which have been sliced into fewer (i.e. larger) stripes, the deviation from the control data was in many case non-significant for the samples cut into narrower stripes. This effect was particularly evident for the 0.1 Gy - 0.5 mm stripe data (Figure 3 top graph panel C), were only the central directly irradiated stripe and the two stripes in close proximity exhibit significant increased micronucleation.

Finally, possible radiation induced cell cycle delay was assessed by monitoring the fraction of binucleated cells recovered. As shown in the table 1 the radiation exposure doesn't appear to affect the fraction of binucleated cells either in the whole sample or in the individual stripe containing the directly irradiated cells.

	% Binucleated Cells
Control (0 Gy)	66.2 ± 6.0
0.1 Gy	62.3 ± 5.6
0.5 Gy	66.0 ± 6.0
1 Gy	66.2 ± 7.4

Table 1. Fraction of average binucleated cells per sample measured with the above described protocol following partial irradiation exposures.

4. **Discussion**

The objective of the work described in this manuscript was to develop a novel assay to measure direct and bystander radiation damage on an *in vitro* 3D human skin tissue model. The use of a biological model that closely resembles normal human tissue offers great potential for the investigation of non-targeted radiation effects in a more relevant environment where cell signalling and direct cell-cell contact play a critical role. Although 3D models have already been used for similar studies, so far it has not been possible to investigate the bystander contribution for induction of critical DNA damage events such as chromosome aberrations and mutations. This was due to difficulty in performing single cell assays in tissues, while preserving their spatial correlation. We have used the described method to investigate the induction of micronuclei following partial irradiation (50 μm wide line across the tissue diameter) with 3.5 MeV protons in order to compare the results with available published data and demonstrate the feasibility of the protocol.

The developed slicing and harvesting protocol has been shown to be able to recover a very large fraction of the tissue cells obtaining a still viable single cell solution. The number of cells recovered was in agreement with the number calculated with a simple geometrical approach and with the estimation provided by the tissue supply company (MatTek). The home built microtome to slice live tissues has proved to be very precise and effective, easy to use and

economically affordable. Three different Cytochalasin-B concentrations have been tested for an incubation time up to 72 h to determine cell division rate and the best conditions for micronuclei scoring. The max number of binucleated cells was achieved for a 3 μg/ml concentration and 48 h incubation with no evident improvement for longer incubations or higher concentrations. Although the fraction of binucleated cells measured (~60%) was lower than that observed in the same *in vitro* cell cultures, it is still adequate to perform the proposed studies and highlights an overall healthy and viable single cell population. Additionally, the background frequency of micronuclei scored in the control samples is considerably low (0.72 ± 0.37 % of micronucleated cells) and very reproducible making the model suitable for straightforward statistical analysis. The lack of increase of micronuclei in control samples which have been slices compared to that measured in intact tissues, also indicates that no considerable stress or alteration is introduced by the slicing process.

Partial irradiation of the samples resulted in an elevated micronuclei frequency not only in the stripes containing the direct irradiated cells but also in the adjacent stripes with unexposed cells. The damage detected in those cells cannot be attributed to the effect of proton scattering ($< \pm 15$ μm as from TRIM simulations) or secondary electrons (max energy ~7.5 keV, range <2.5 μm). The magnitude of the bystander effect observed seems to be dose independent and clearly detectable in our 3D tissue models for doses as low as 0.1 Gy. Furthermore, the data indicate a higher level of micronuclei in the central portion of the sample (i.e. closer to the irradiation site) with evidence of a decreasing but still detectable effect towards the edges. This suggests a range for the bystander response of several millimetres with potential critical consequences for radiotherapy and radioprotection as it essentially increases the volume and the number of cells affected. The higher fraction of micronuclei detected in the central area of the sample and the very long range of the effect, support the hypothesis that signal(s) are generated by the cells directly damaged by radiation and propagate cell-by-cell (whatever they will be damaged or not) with great efficiency. Due to the overall low level of damage induced (<3 % micronucleated cells), if the bystander signal were to be propagated only by the damaged cells (although with high efficiency), it would have been reasonable to expect a rapid decrease with distance from the irradiation site. The long range of the effect seems to suggest that cells that do not exhibit damage are also involved in the signal propagation.

Interestingly, almost no significant increase above the background level was measured for the 0.1 Gy - 0.5 mm stripes dose point. A possible explanation could lie in the different number of cells scored (~1000 samples for the narrow stripes against more than 2000 for all other cases) as forced by the lower number of cells recovered. However under the same experimental conditions (0.5 mm wide stripes), significant bystander effect was detected for the 1 Gy dose point with the 0.5 Gy relative data showing an ambiguous response. Further investigations are required by expanding the dose range and/or by slicing the samples into finer stripes.

V. References

Belyakov O.V., Mitchell S.A., Parikh D., Randers-Pehrson G., Marino S.A., Amundson S.A., Geard C.R. and Brenner D.J. Biological effects in unirradiated human tissue induced by radiation damage up to 1 mm away. PNAS 102:14203-14208 (2005)

Mitchell S.A., Marino S.A., Brenner D.J. and Hall E.J. Bystander effect and adaptive response in C3H 10T1/2 cells. Int. J. Radiat. Biol. 80:465-472 (2004).

Mitchell S.A., Randers-Pehrson G., Brenner D.J. and Hall E.J. The Bystander Response in C3H 10T(1/2) Cells: The Influence of Cell-to-Cell Contact. Radiat. Res. 161:397-401 (2004).

Schettino G., Johnson G.W., Marino S.A. and Brenner D.J. Development of a method for assessing non-targeted radiation damage in an artificial 3D human skin model. Radiat. Res. Submitted (2009).